0090-9556/08/3609-1819–1827$20.00
DRUG METABOLISM AND DISPOSITION
Vol. 36, No. 9
21154/3372212
Printed in U.S.A.

DMD 36:1819–1827, 2008

Down-Regulation of the Carcinogen-Metabolizing Enzyme Cytochrome P450 1a1 by Vanadium

Anwar Anwar-Mohamed and Ayman O. S. El-Kadi

Faculty of Pharmacy and Pharmaceutical Sciences, University of Alberta, Edmonton, Alberta, Canada

Received February 20, 2008; accepted June 4, 2008

ABSTRACT:

Vanadium (V^{5+}), a heavy metal contaminant with important toxicological consequences, has received considerable attention as an anticancer agent, although the mechanisms remain unknown. As a first step to investigate these mechanisms, we examined the effect of V^{5+} (as ammonium metavanadate, NH_4VO_3) on the expression of the aryl hydrocarbon receptor (AhR)-regulated gene: cytochrome P450 1a1 (*Cyp1a1*) at each step of the AhR signal transduction pathway, using Hepa 1c1c7 cells. Our results showed a significant reduction in 2,3,7,8-tetrachlorodibenzo-*p*-dioxin (TCDD)-mediated induction of Cyp1a1 mRNA, protein and activity levels after V^{5+} treatments in a dose-dependent manner. Investigation of the effect of coexposure to V^{5+} and TCDD at transcriptional levels revealed that V^{5+} significantly inhibited TCDD-mediated induction of AhR-dependent luciferase reporter gene expression. Furthermore, despite not affecting the direct activation of the cytosolic AhR by TCDD and subsequently transforming it to a DNA-binding form, V^{5+} inhibited the nuclear accumulation of liganded AhR and subsequent formation of the AhR/aryl hydrocarbon nuclear translocator (Arnt)/xenobiotic responsive element (XRE) complex. Importantly, the V^{5+}-mediated inhibition of AhR/Arnt/XRE complex formation coincided with a significant decrease in ecto-ATPase activity. Looking at the post-transcriptional and post-translational effects of V^{5+} on existing Cyp1a1 mRNA and protein levels, we showed that V^{5+} did not affect Cyp1a1 mRNA or protein stability, thus eliminating possible role of V^{5+} in modifying *Cyp1a1* gene expression through these mechanisms. This study provides the first evidence that V^{5+} down-regulates the expression of Cyp1a1 at the transcriptional level through an ATP-dependent mechanism.

The aryl hydrocarbon receptor (AhR) is a ligand-activated cytoplasmic transcription factor that belongs to the basic-helix-loop-helix protein family. The inactive form of AhR is attached to a complex of two heat shock proteins 90 (HSP90), hepatitis B virus X-associated protein (XAP2), and the chaperone protein p23 (Hankinson, 1995; Meyer et al., 1998). Upon ligand binding, the AhR-ligand complex dissociates from the cytoplasmic complex and translocates to the nucleus where it associates with the aryl hydrocarbon nuclear translocator (Arnt) (Whitelaw et al., 1994). The whole complex then acts as a transcription factor that binds to a specific DNA recognition sequence, termed the xenobiotic responsive element (XRE), located in the promoter region of a number of AhR-regulated genes (Denison et al., 1989; Nebert et al., 2004). Among these genes are those encoding a number of drug-metabolizing enzymes, including four phase I enzymes: cytochrome P450 1a1 (Cyp1a1), Cyp1a2, Cyp1b1, and Cyp2s1; and four phase II enzymes: NAD(P)H:quinone oxidoreductase-1, glutathione *S*-transferase a1, cytosolic aldehyde dehydrogenase-3, and UDP-glucuronosyltransferase 1a6 (Nebert and Duffy, 1997).

Experimental and epidemiological data have shown that various environmental pollutants such as halogenated aromatic hydrocarbons are capable of producing a variety of toxic effects in exposed organisms; some of the most common toxicities include neurotoxicity, immune dysfunction, reproductive and developmental effects, and cancer (Schrenk, 1998; Elbekai and El-Kadi, 2004). Mounting evidence suggests that most of the toxic manifestations induced by, 2,3,7,8-tetrachlorodibenzo-*p*-dioxin (TCDD), the most toxic halogenated aromatic hydrocarbon with the greatest affinity for AhR, are occurring through the activation of the AhR (Kransler et al., 2007). As a result of the tight correlation between AhR binding affinity and Cyp1a1 induction, Cyp1a1 has been used as a biomarker for evaluating hazards and risk assessments of environmental pollutants (Behnisch et al., 2001). By itself, Cyp1a1 is capable of producing polar, toxic, or even carcinogenic metabolites from various AhR ligands including aromatic and halogenated hydrocarbons (Anwar-Mohamed and El-Kadi, 2007).

The toxicity of individual AhR ligands has been examined in numerous studies, yet the combined toxic effects of these ligands and other environmental cocontaminants typified by heavy metals such as vanadium (V^{5+}) are still unclear. V^{5+}, a cocontaminant with AhR

This work was supported by Natural Sciences and Engineering Research Council of Canada Discovery Grant RGPIN 250139-07 to A.O.S.E.-K. A.A.-M. is recipient of a Mike Wolowyk Graduate Scholarship award.

Article, publication date, and citation information can be found at http://dmd.aspetjournals.org.

doi:10.1124/dmd.108.021154.

ABBREVIATIONS: AhR, aryl hydrocarbon receptor; Arnt, aryl hydrocarbon receptor nuclear translocator; XRE, xenobiotic responsive element; Cyp1a1, cytochrome P450 1a1; TCDD, 2,3,7,8-tetrachlorodibenzo-*p*-dioxin; V^{5+}, vanadium; pGudluc1.1, XRE-luciferase reporter plasmid; EMSA, electrophoretic mobility shift assay; MTT, 3-(4,5-dimethylthiazol-2-yl)-2,5-diphenyltetrazolium bromide; CHX, cycloheximide; Act-D, actinomycin D; DMSO, dimethylsulfoxide; PBS, phosphate-buffered saline; PCR, polymerase chain reaction; HO-1, heme oxygenase-1; PAGE, polyacrylamide gel electrophoresis; Gapdh, glyceraldehyde-3-phosphate dehydrogenase; EROD, 7-ethoxyresorufin *O*-deethylase; NF-κB, nuclear factor-κB.

ligands, is widely distributed in nature. The oxidation state of V (+4 or + 5) seems to be important for its actions on enzymes (Cantley and Aisen, 1979). V^{5+} compounds have been found in various types of food, such as black pepper, mushrooms, dill seed, parsley, and shellfish (Rojas et al., 1999). Interestingly, previous studies have demonstrated that V^{5+} compounds exert protective effects against chemical-induced carcinogenesis mainly by modifying various xenobiotic-metabolizing enzymes; however, the exact mechanism(s) remain unknown (Evangelou, 2002).

The objective of this study was to determine the effect of coexposure to V^{5+} and TCDD on Cyp1a1 and to investigate the molecular mechanisms involved. As a first step in investigating these mechanisms, we examined the effect of coexposure to V^{5+} and TCDD on Cyp1a1 mRNA, protein, and activity levels in Hepa 1c1c7 cells. To address whether the observed effects of coexposure to V^{5+} and TCDD occurred through an AhR-dependent mechanism, we examined the effect of the coexposure on luciferase activity in Hepa 1c1c7 cells transiently transfected with the XRE-driven luciferase plasmid pGudLuc1.1. Looking at the involvement of post-transcriptional mechanisms, we tested the effect of V^{5+} on Cyp1a1 mRNA and protein stability. We also examined the ability of V^{5+} to modulate AhR/Arnt/XRE binding using the electrophoretic mobility shift assay (EMSA) and the role of ecto-ATPase in this modulation. We provide here the first evidence that V^{5+} down-regulates the expression of Cyp1a1 by inhibiting the translocation of the transformed AhR, possibly through an ATP-dependent mechanism.

Materials and Methods

Materials. Ammonium metavanadate (NH_4VO_3), 3-(4,5-dimethylthiazol-2-yl)-2,5-diphenyltetrazolium bromide (MTT), cycloheximide (CHX), *p*-nitrophenyl phosphate, *p*-nitrophenol, 2,6-dichlorophenolindophenol, 7-ethoxyresorufin, fluorescamine, anti-goat IgG peroxidase secondary antibody, and protease inhibitor cocktail were purchased from Sigma-Aldrich (St. Louis, MO). 2,3,7,8-Tetrachlorodibenzo-*p*-dioxin, >99% pure, was purchased from Cambridge Isotope Laboratories (Woburn, MA). TRIzol reagent and Lipofectamine 2000 reagents were purchased from Invitrogen (San Diego, CA). The High-Capacity cDNA Reverse Transcription Kit and SYBR Green PCR Master Mix were purchased from Applied Biosystems (Foster City, CA). Actinomycin-D (Act-D) was purchased from Calbiochem (San Diego, CA). Chemiluminescence Western blotting detection reagents were from GE Healthcare Life Sciences (Piscataway, NJ). Nitrocellulose membrane was purchased from Bio-Rad (Hercules, CA). Cyp1a1 goat polyclonal primary antibody, AhR rabbit polyclonal primary antibody, and anti-rabbit IgG peroxidase secondary antibody were purchased from Santa Cruz Biotechnology, Inc. (Santa Cruz, CA). Luciferase assay reagents were obtained from Promega (Madison, WI). [γ-^{32}P]ATP was supplied by the DNA Core Services Laboratory, University of Alberta. All other chemicals were purchased from Thermo Fisher Scientific (Toronto, ON, Canada).

Cell Culture. The Hepa 1c1c7 cell line (number CRL-2026; American Type Culture Collection, Manassas, VA), was maintained in Dulbecco's modified Eagle's medium without phenol red and supplemented with 10% heat-inactivated fetal bovine serum, 20 μM *l*-glutamine, 50 μg/ml amikacin, 100 IU/ml penicillin, 10 μg/ml streptomycin, 25 ng/ml amphotericin B, 0.1 mM nonessential amino acids, and vitamin supplement solution. Cells were grown in 75-cm^2 cell culture flasks at 37°C in a 5% CO_2 humidified incubator.

Chemical Treatments. Cells were treated in serum-free medium with various concentrations of V^{5+} (25–1000 μM) in the absence and presence of 1 nM TCDD as described in the figure legends. TCDD was dissolved in dimethyl sulfoxide (DMSO) and maintained in DMSO at −20°C until use. V^{5+} was prepared freshly in double deionized water. In all treatments, the DMSO concentration did not exceed 0.05% (v/v).

Effect of V^{5+} on Cell Viability. The effect of V^{5+} on cell viability was determined using the MTT and ATP-based luminescent assays as described previously (Maniratanachote et al., 2005; Korashy and El-Kadi, 2008). The MTT assay measures the conversion of MTT to formazan in living cells via mitochondrial enzymes of viable cells. In brief, Hepa 1c1c7 cells were seeded into 96-well microtiter cell culture plates and incubated for 24 h at 37°C in a 5% CO_2 humidified incubator. Cells were treated with various concentrations of V^{5+} (25–1000 μM) in the absence and presence of 1 nM TCDD. After 24 h of incubation, the medium was removed and replaced with cell culture medium containing 1.2 mM MTT dissolved in phosphate-buffered saline (PBS) (pH 7.4). After 2 h of incubation, the formed crystals were dissolved in isopropanol. The intensity of the color in each well was measured at a wavelength of 550 nm using the Bio-Tek EL 312e microplate reader (Bio-Tek Instruments, Winooski, VT).

The ATP-based luminescent assay measures the quantity of the ATP produced by metabolically active cells, which was determined using a CellTiter-Glo Luminescent assay kit according to the manufacturer's instructions (Promega). In brief, Hepa 1c1c7 cells were seeded into 24-well cell culture plates and incubated for 24 h at 37°C in a 5% CO_2 humidified incubator. Cells were then treated with various concentrations of V^{5+} (25–1000 μM) in the absence and presence of 1 nM TCDD for another 24 h. At the end of treatment period, 200 μl of CellTiter-Glo reagent was added to each well. The luminescent signal generated was monitored on a TD-20/20 luminometer (Turner BioSystems, Sunnyvale CA).

RNA Extraction and Quantitative Real-Time PCR of Cyp1a1. After incubation with the test compounds for the specified time periods, total cellular RNA was isolated using TRIzol reagent, according to manufacturer's instructions (Invitrogen), and quantified by measuring the absorbance at 260 nm. For reverse transcription-PCR, first-strand cDNA was synthesized from 1.0 μg of total RNA using the High-Capacity cDNA Reverse Transcription Kit with random primers. Real-time PCR reactions were performed on an ABI 7500 real-time PCR system (Applied Biosystems), using SYBR Green PCR Master Mix. The amplification reactions were performed as follows: 10 min at 95°C and 40 cycles of 94°C for 15 s and 60°C for 1 min. Primers and probes as follows were purchased from Integrated DNA Technologies, Inc. (Coralville, IA): for mouse Cyp1a1 forward primer 5′-GGT TAA CCA TGA CCG GGA ACT-3′ and reverse primer 5′-TGC CCA AAC CAA AGA GAG TGA-3′; for heme oxygenase-1(HO-1) forward primer 5′-GTG ATG GAG CGT CCA CAG C-3′ and reverse primer 5′-TGG TGG CCT CCT TCA AGG-3′; and for β-actin forward primer 5′-TAT TGG CAA CGA GCG GTT CC-3′ and reverse primer 5′-GGC ATA GAG GTC TTT ACG GAT GTC-3′. The fold change in the level of Cyp1a1 (target gene) between treated and untreated cells, corrected by the level of β-actin, was determined using the following equation: fold change $= 2^{-\Delta(\Delta C_t)}$, where $\Delta C_t = C_{t\,(\text{target})} - C_{t\,(\beta\text{-actin})}$ and $\Delta(\Delta C_t) = \Delta C_{t\,(\text{treated})} - \Delta C_{t\,(\text{untreated})}$.

Protein Extraction and Western Blot Analysis. Twenty-four hours after incubation with the test compounds, cells were collected in lysis buffer containing 50 mM HEPES, 0.5 M sodium chloride, 1.5 mM magnesium chloride, 1 mM EDTA, 10% (v/v) glycerol, 1% Triton X-100, and 5 μl/ml of protease inhibitor cocktail. The cell homogenates were obtained by incubating the cell lysates on ice for 1 h, with intermittent vortexing every 10 min, followed by centrifugation at 12,000*g* for 10 min at 4°C. Proteins (25 μg) were resolved by denaturing electrophoresis, as described previously (Elbekai and El-Kadi, 2004). Briefly, the cell homogenates were dissolved in 1× sample buffer, boiled for 5 min, separated by 10% SDS-PAGE and electrophoretically transferred to a nitrocellulose membrane. Protein blots were blocked for 24 h at 4°C in blocking buffer containing 5% skim milk powder, 2% bovine serum albumin, and 0.05% (v/v) Tween 20 in Tris-buffered saline solution (0.15 M sodium chloride, 3 mM potassium chloride, and 25 mM Tris base). After blocking, the blots were incubated with a primary polyclonal goat anti-mouse Cyp1a1 antibody for 2 h at room temperature or primary polyclonal rabbit anti-mouse AhR antibody overnight at 4°C in Tris-buffered saline containing 0.05% (v/v) Tween 20 and 0.02% sodium azide. Incubation with a peroxidase-conjugated rabbit anti-goat IgG secondary antibody for Cyp1a1 and Gapdh or goat anti-rabbit IgG for AhR was carried out in blocking buffer for 1 h at room temperature. The bands were visualized with the enhanced chemiluminescence method according to the manufacturer's instructions (GE Healthcare, Mississauga, ON). The intensity of Cyp1a1 protein bands was quantified relative to the signals obtained for Gapdh protein, using ImageJ software.

Determination of Cyp1a1 Enzymatic Activity. Cyp1a1-dependent 7-ethoxyresorufin *O*-deethylase (EROD) activity was performed on intact, living cells using 7-ethoxyresorufin as a substrate, as described previously

(Elbekai and El-Kadi, 2004). Enzymatic activity was normalized for cellular protein content, which was determined using a modified fluorescent assay (Lorenzen and Kennedy, 1993).

Transient Transfection and Luciferase Assay. Hepa 1c1c7 cells were plated onto six-well cell culture plates. Each well of cells was transfected with 4 μg of XRE-driven luciferase reporter plasmid pGudLuc1.1 using Lipofectamine 2000 reagent according to the manufacturer's instructions (Invitrogen). The luciferase assay was performed according to the manufacturer's instructions (Promega) as described previously (Elbekai and El-Kadi, 2007). In brief, after incubation with test compounds for 24 h, cells were washed with PBS, 200 μl of 1× lysis buffer was added into each well with continuous shaking for at least 20 min, and then the content of each well was collected separately in 1.5-ml microcentrifuge tubes. The tubes were then centrifuged to precipitate cellular waste, 100 μl of cell lysate was incubated with 100 μl of stabilized luciferase reagent, and luciferase activity was quantified using a TD-20/20 luminometer (Turner BioSystems).

EMSA. Nuclear extracts were prepared from Hepa 1c1c7 cells and treated for 2 h with vehicle, 5 nM TCDD, in the absence and presence of 50 μM V^{5+} using the method of Denison et al. (2002). Because of the low efficiency of transformation of the mouse AhR, resulting from the extreme resistance of HSP90 to dissociate from the mouse AhR, compared with the greatest degree of transformation of the guinea pig AhR in response to AhR ligand (Bohonowych and Denison, 2007), we used guinea pig cytosol as a model. Therefore, hepatic cytosol of untreated guinea pig, generously provided by Dr. M. S. Denison at University of California, Davis (Davis, CA), was incubated with the test compounds for a final concentration of 20 nM TCDD, in the absence and presence of 100 and 250 μM V^{5+} for 2 h at 20°C. Protein concentrations for the nuclear and cytosolic extracts were determined using the method of Lowry et al. (1951). To visualize the ability of V^{5+} to alter the transformation and subsequent DNA binding of the AhR, a complementary pair of synthetic oligonucleotides containing the sequences 5′-GAT CTG GCT CTT CTC ACG CAA CTC CG-3′ and 5′-GAT CCG GAG TTG CGT GAG AAG AGC CA-3′, corresponding to the XRE binding site, were synthesized and radiolabeled with [γ-^{32}P]ATP as described previously (Denison et al., 2002) and used as a DNA probe in all experiments. Binding reactions using aliquots of 120 μg of cytosolic or 20 μg of nuclear extracts and excess radiolabeled oligonucleotides were allowed to proceed for 15 min at 20°C in a buffer containing 1 mM EDTA, 1 mM dithiothreitol, 10% glycerol, 25 mM HEPES, 400 ng to 2 μg of poly(dI-dC), and 0.4 to 0.8 mM KCl. To determine the specificity of binding to the oligonucleotide, a 100-fold molar excess of unlabeled XRE probe was added to the binding reaction before addition of the γ-^{32}P-labeled probe. Protein-DNA complexes were separated under nondenaturing conditions on a 4% polyacrylamide gel using 1× TBE (90 mM Tris borate, 90 mM boric acid, and 4 mM EDTA) as a running buffer. The gels were dried and the protein-DNA complexes were visualized by autoradiography.

Cyp1a1 mRNA Stability. The half-life of Cyp1a1 mRNA was analyzed by an Act-D chase assay. Cells were pretreated with 1 nM TCDD for 12 h. Cells were then washed and incubated with 5 μg/ml Act-D to inhibit further RNA synthesis, immediately before treatment with 50 μM V^{5+}. Total RNA was extracted at 0, 1, 3, 6, and 12 h after incubation with the metal. Real-time PCR reactions were performed using SYBR Green PCR Master Mix. The fold change in the level of Cyp1a1 (target gene) between treated and untreated cells, corrected by the level of β-actin, was determined using the following equation: fold change $= 2^{-\Delta(\Delta C_t)}$, where $\Delta C_t = C_{t\,(\text{target})} - C_{t\,(\beta\text{-actin})}$ and $\Delta(\Delta C_t) = \Delta C_{t\,(\text{treated})} - \Delta C_{t\,(\text{untreated})}$.

Cyp1a1 Protein Stability. The half-life of Cyp1a1 protein was analyzed by the CHX chase assay. Cells were pretreated with 1 nM TCDD for 24 h. Cells were then washed and incubated with 10 μg/ml CHX, to inhibit further protein synthesis, immediately before treatment with 50 μM V^{5+}. Cell homogenates were extracted at 0, 1, 3, 6, and 12 h after incubation with the metal. Cyp1a1 protein was measured by Western blotting. The intensity of Cyp1a1 protein bands was quantified, relative to the signals obtained for Gapdh protein, using ImageJ software. The protein half-life values were determined from semilog plots of integrated densities versus time.

Determination of Total Cellular Heme Content. Cellular heme content was determined by a modification of the method of Ward et al. (1984). After a 24-h incubation period with 50 μM V^{5+} in the absence and presence of 1 nM TCDD, cells were pelleted and boiled in 2.0 M oxalic acid for 30 min followed by resuspension in cold PBS and centrifugation at 14,000*g* for 15 min. The supernatant was then removed and the fluorescence of protoporphyrin IX was assayed using the Eclipse fluorescence spectrophotometer (Varian Australia PTY Ltd., Melbourne, Australia) using an excitation wavelength of 405 nm and an emission wavelength of 600 nm. Background was determined by measuring the fluorescence in the absence of cells. Cellular heme content was calculated as a percentage of serum-free medium treated cells after normalization of cellular heme content with cellular protein, which was determined using the method of Lowry et al. (1951).

Determination of Ecto-ATPase Enzymatic Activity. To examine the effect of V^{5+} on ecto-ATPase activity, a colorimetric method using the conversion of *p*-nitrophenyl phosphate to *p*-nitrophenol was used as described previously (Anagnostou et al., 1996). In brief, cells were seeded in 12-well plates for 48 h. Thereafter, the cells were treated with vehicle, V^{5+}, TCDD, or V^{5+} plus TCDD for 6 h. Cells were then washed with phosphate-free buffer (15 mM Tris, 134 mM NaCl, 3 mM $CaCl_2$, and 3 mM $MgCl_2$), pH 8.0, and the medium was replaced with 1 ml of 0.5 mM *p*-nitrophenyl phosphate and incubated for 2 h at 37°C. To stop the reaction, 1 ml of 0.2 M NaOH was added to each well. Thereafter, the cells were harvested and centrifuged at 14,000*g* for 5 min. *p*-Nitrophenol in the supernatant was quantified by measuring the absorbance at 405 nm. Enzymatic activity was normalized for cellular protein content, which was determined using the assay of Lowry et al. (1951).

Statistical Analysis. The comparative analysis of the results from various experimental groups with their corresponding controls was performed using SigmaStat for Windows (Systat Software, Inc., San Jose, CA). A one-way analysis of variance followed by the Student-Newman-Keul test was carried out to assess statistical significance. The differences were considered significant when $p < 0.05$.

Results

Effect of Coexposure to V^{5+} and TCDD on Cell Viability. To determine the maximum nontoxic concentrations of V^{5+} to be used in the current study, Hepa 1c1c7 cells were exposed for 24 h to increasing concentrations of V^{5+} (25–1000 μM) in the absence and presence of 1 nM TCDD. Thereafter, cytotoxicity was assessed using MTT and CellTiter-Glo Luminescent assays.

Figure 1A shows that V^{5+} alone at concentrations of 25 to 250 μM did not affect cell viability; however, the highest concentration, 1000 μM, decreased cell viability to approximately 67%. Similarly coexposure to V^{5+} and TCDD produced a significant decrease in cell viability, at the highest concentration tested (1000 μM), to approximately 70%. On the other hand, the concentration-dependent effect of exposure to V^{5+} in the absence and presence of 1 nM TCDD using the CellTiter-Glo Luminescent assay exhibited a pattern relatively similar to that observed with the MTT experiment (Fig. 1B). Therefore, all subsequent studies were conducted using concentrations of 25 to 250 μM in the absence and presence of 1 nM TCDD.

Concentration-Dependent Effect of Coexposure to V^{5+} and TCDD on Inducible Cyp1a1 mRNA. To better understand the kinetics of Cyp1a1 in response to coexposure to V^{5+} and TCDD, Hepa 1c1c7 cells were treated with various concentrations of V^{5+} (Fig. 2). Thereafter, Cyp1a1 mRNA was assessed using real-time PCR. TCDD alone caused a 38-fold increase in Cyp1a1 mRNA that was inhibited in a dose-dependent manner by V^{5+}, starting at a concentration of 25 μM and reaching maximum inhibition at the concentration of 250 μM (Fig. 2).

Concentration-Dependent Effect of Coexposure to V^{5+} and TCDD on Cyp1a1 Protein and Catalytic Activity. To examine whether the observed inhibition of the TCDD-mediated induction of Cyp1a1 mRNA is reflected at the protein and activity levels, Hepa 1c1c7 cells were treated for 24 h with increasing concentrations of V^{5+} in the absence and presence of 1 nM TCDD. Figure 3, A and B, show that TCDD alone caused 20- and 35-fold increases in Cyp1a1 protein and catalytic activity, respectively. On the other hand, V^{5+}

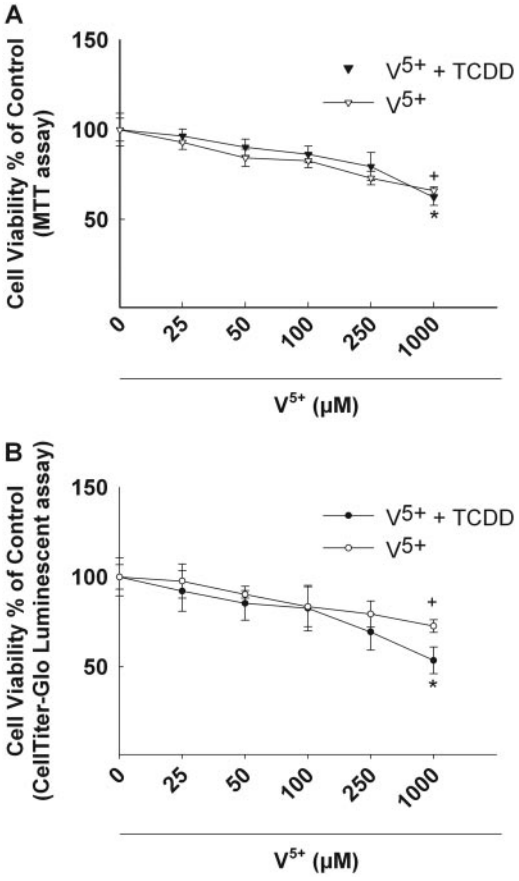

FIG. 1. Effect of V^{5+} on cell viability. Hepa 1c1c7 cells were treated for 24 h with V^{5+} (0, 25, 50, 100, 250, and 1000 μM) in the absence and presence of 1 nM TCDD. Cell cytotoxicity was determined using MTT (A). and CellTiter-Glo Luminescent (B) assays. Data are expressed as percentage of untreated control (which is set at 100%) ± S.E. (n = 8). +, $P < 0.05$, compared with control (concentration = 0 μM); ∗, $P < 0.05$, compared with the respective TCDD treatment.

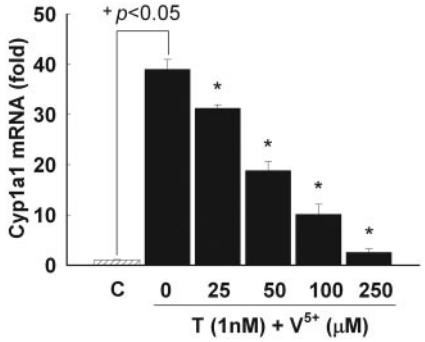

FIG. 2. Effect of V^{5+} on Cyp1a1 mRNA using real-time PCR. Hepa 1c1c7 cells were treated for 6 h with increasing concentrations of V^{5+} in the presence of 1 nM TCDD. First-strand cDNA was synthesized from total RNA (1 μg) extracted from Hepa 1c1c7 cells. cDNA fragments were amplified and quantitated using an ABI 7500 real-time PCR system as described under *Materials and Methods*. Duplicate reactions were performed for each experiment, and the values presented are the means of three independent experiments. +, $P < 0.05$, compared with control (C) (concentration = 0 μM); ∗, $P < 0.05$, compared with the respective TCDD (T) treatment.

significantly reduced the TCDD-mediated induction of Cyp1a1 protein and activity levels in a dose-dependent manner. This inhibition pattern was consistent with that observed at mRNA levels, in which the initial significant inhibition took place with 50 μM V^{5+}, and maximal inhibition was reached at 250 μM (Fig. 3, A and B).

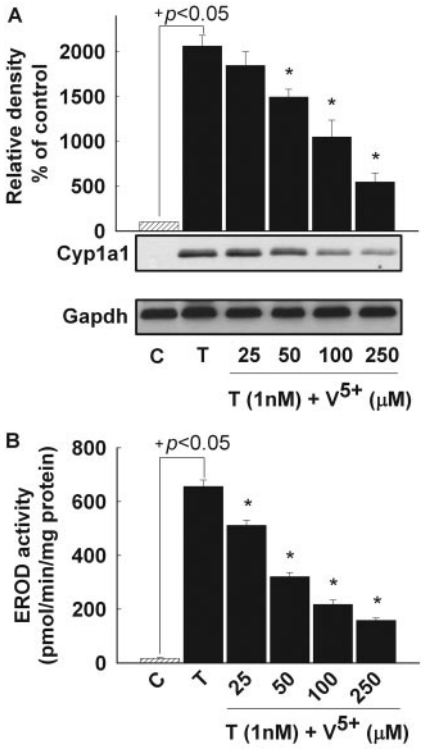

FIG. 3. Effect of V^{5+} on inducible Cyp1a1 protein and EROD activity. Hepa 1c1c7 cells were treated for 24 h with increasing concentrations of V^{5+} in the presence of 1 nM TCDD. A, protein (25 μg) was separated by 10% SDS-PAGE and transferred to a nitrocellulose membrane. Protein blots were then blocked overnight at 4°C and incubated with a primary Cyp1a1 antibody for 2 h at 4°C, followed by a 1-h incubation with secondary antibody at room temperature. Cyp1a1 protein was detected using the enhanced chemiluminescence method. The intensity of bands was normalized to Gapdh signals, which was used as a loading control. One of three representative experiments is shown. B, EROD activity was measured in intact living cells treated with increasing concentrations of V^{5+}, in the absence and presence of 1 nM TCDD for 24 h. Cyp1a1 activity was measured using 7-ethoxyresorufin as a substrate. Values are presented as mean ± S.E. (n = 8). +, $P < 0.05$, compared with control (C); ∗, $P < 0.05$, compared with the respective TCDD (T) treatment.

Transcriptional Inhibition of Cyp1a1 Gene Induction by V^{5+}. To investigate whether the observed effect upon coexposure to V^{5+} and TCDD on Cyp1a1 is occurring through an AhR-dependent mechanism, Hepa 1c1c7 cells were transiently transfected with the XRE-driven luciferase reporter gene to study the effect of V^{5+} on the AhR-dependent transcriptional activation. Luciferase activity results showed that 50 μM V^{5+} alone did not alter the luciferase activity (Fig. 4). In contrast, 1 nM TCDD alone was capable of causing a significant induction of the luciferase activity that reached up to 1200 relative light units, compared with control. On the other hand, co-treatment with V^{5+} and TCDD significantly decreased the luciferase activity by 3-fold compared with TCDD alone (Fig. 4).

In an effort to determine whether V^{5+} interferes with the nuclear binding of the transformed AhR to the XRE, we examined the potential effect of V^{5+} on TCDD-induced translocation of the AhR to the nucleus and subsequent binding to XRE, the promoter sequence of Cyp1a1, by EMSA. For this purpose, Hepa 1c1c7 cells were treated with vehicle, V^{5+}, TCDD, or V^{5+} plus TCDD for 1 h, followed by extraction of nuclear extracts. Extracts from vehicle- and TCDD-treated cells were used as negative and positive controls, respectively. Figure 5A shows that V^{5+} alone did not induce AhR/Arnt/XRE complex formation, as shown by the intensity of the bands. In contrast, TCDD significantly increased AhR/Arnt/XRE binding. In addition, V^{5+} completely abolished the TCDD-induced nuclear formation

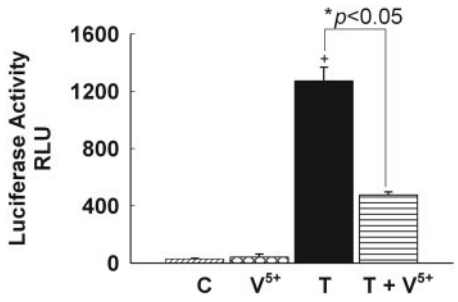

FIG. 4. Effect of V^{5+} on luciferase activity. Hepa 1c1c7 cells were transiently transfected with the XRE-luciferase transporter plasmid pGudLuc1.1. Cells were treated with vehicle, TCDD (1 nM), V^{5+} (50 μM), or TCDD (1 nM) + V^{5+} (50 μM) for 24 h. Cells were lysed, and luciferase activity was measured according to the manufacturer's instruction. Luciferase activity is reported as relative light units (RLU). Values are presented as mean ± S.E. ($n = 6$). +, $P < 0.05$, compared with control (C); *, $P < 0.05$, compared with the respective TCDD (T) treatment.

of AhR/Arnt/XRE complex (lane 3). The specificity of the TCDD-induced AhR/Arnt heterodimer binding to XRE was confirmed by a competition assay using a 100-fold molar excess of unlabeled XRE.

To examine the ability of V^{5+} to inhibit direct activation of the cytosolic AhR by TCDD and subsequent DNA binding, EMSA was performed on untreated guinea pig hepatic cytosol incubated with vehicle, V^{5+}, TCDD, or V^{5+} plus TCDD for 2 h in vitro. Figure 5B shows that V^{5+} alone, at the indicated concentrations, failed to induce the AhR/Arnt/XRE complex transformation, as determined by the shifted band, compared with TCDD alone. Furthermore, V^{5+} did not inhibit the TCDD-induced transformation of the AhR/Arnt/XRE complex. Collectively, our data indicate that V^{5+} inhibited the translocation process rather than inhibiting the binding step in the AhR transduction pathway.

Time-Dependent Effect of Coexposure to V^{5+} and TCDD on AhR Protein. To determine whether the V^{5+} effect on Cyp1a1 is due to increasing AhR protein degradation, we examined the effect of coexposure to V^{5+} and TCDD on the AhR protein using total cell lysate over a 24-h time course. Our results showed that AhR is a short-lived protein with only 15% of AhR protein remained at 6 h after TCDD treatment (Fig. 6). On the other hand, coexposure to V^{5+} and TCDD did not significantly alter the AhR protein level compared with TCDD alone. These results exclude the possibility that V^{5+} may alter the Cyp1a1 by lowering the cellular levels of AhR protein.

Post-Transcriptional Modification of Cyp1a1 mRNA by V^{5+}. The level of mRNA expression is not only a function of the transcription rate but is also dependent on the elimination rate, through processing or degradation. Previous reports from our laboratory have shown that various heavy metals modulate the expression of the Cyp1a1 through transcriptional and post-transcriptional mechanisms (Korashy and El-Kadi, 2005; Elbekai and El-Kadi, 2007). Therefore, we examined the effect of V^{5+} on the stability of Cyp1a1 mRNA transcripts, using an Act-D chase experiment. If V^{5+} alters Cyp1a1 mRNA stability, a decrease in half-life would be expected. Figure 7 shows that Cyp1a1 mRNA decayed with a half-life of 4.73 ± 0.54 h. Furthermore, V^{5+} did not alter the half-life of Cyp1a1 mRNA, indicating that the decrease in Cyp1a1 mRNA transcripts in response to V^{5+} was not due to increasing its degradation.

Post-Translational Modification of Cyp1a1 Protein by V^{5+}. The fact that V^{5+} inhibited TCDD-mediated induction of Cyp1a1 protein raised the question of whether V^{5+} could modify Cyp1a1 protein stability. Therefore, the effect of V^{5+} on Cyp1a1 protein half-life was determined using CHX chase experiments. Figure 8 shows that Cyp1a1 protein induced by TCDD degraded with a half-life of 8.41 ± 0.29 h. Interestingly, V^{5+} did not alter the stability of Cyp1a1 protein (Fig. 8), implying that V^{5+} did not affect Cyp1a1 protein at the post-translational level.

Effect of Coexposure to V^{5+} and TCDD on HO-1 mRNA and Total Cellular Heme Content. We have reported previously that heavy metals other than V^{5+} were able to modify Cyp1a1 by affecting its heme content (Korashy and El-Kadi, 2005; Elbekai and El-Kadi, 2007). Therefore, in the current study we examined the effect of V^{5+} on HO-1 mRNA, a rate-limiting enzyme of heme degradation, and total cellular heme content. For this purpose, Hepa 1c1c7 cells were treated with 50 μM V^{5+} in the absence and presence of 1 nM TCDD (Fig. 9A). Thereafter, HO-1 mRNA was assessed using real-time PCR. Figure 9A shows that V^{5+} and TCDD alone did not alter HO-1 mRNA level. Similarly, coexposure to V^{5+} and TCDD did not significantly alter the HO-1 mRNA level. To confirm the effect of coexposure to V^{5+} and TCDD on heme degradation, we examined the effect of this coexposure on total cellular heme content. Total cellular heme content was measured in Hepa 1c1c7 cells 24 h after treatment with 50 μM V^{5+} in the absence and presence of 1 nM TCDD. Our results show that neither V^{5+} nor TCDD was able to decrease total cellular heme content. Furthermore, coexposure to V^{5+} and TCDD

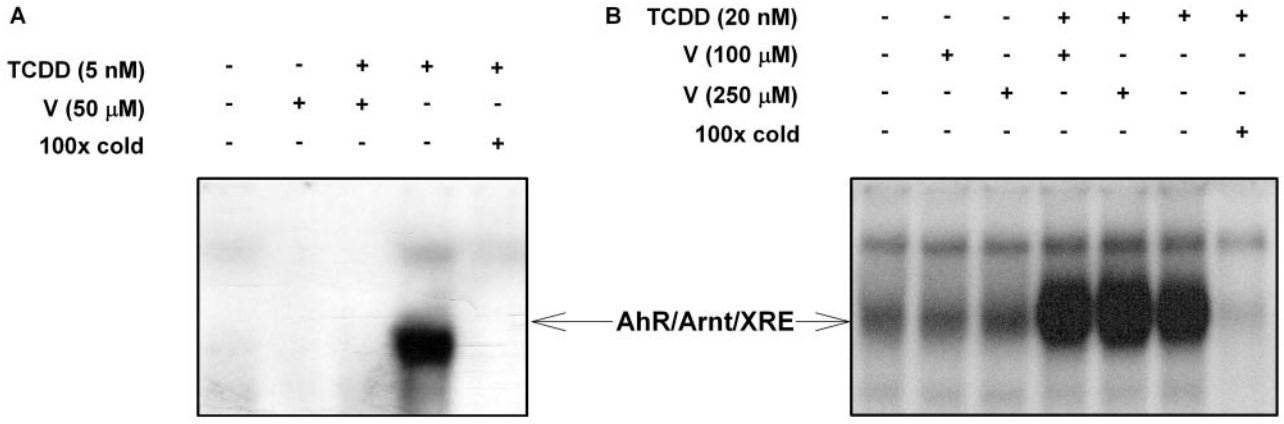

FIG. 5. Effect of V^{5+} on AhR/Arnt/XRE binding. A, nuclear extracts (20 μg) from Hepa 1c1c7 cells were treated for 2 h with vehicle, TCDD (5 nM), V^{5+} (50 μM), or TCDD (5 nM) + V^{5+} (50 μM). B, cytosolic extracts (80 μg) from untreated guinea pig liver extracts were incubated for 2 h with vehicle, TCDD (20 nM), V^{5+} (100 μM), V^{5+} (250 μM), TCDD (20 nM) + V^{5+} (100 μM), or TCDD (20 nM) + V^{5+} (250 μM). The cytosolic and nuclear proteins were mixed with γ-^{32}P-labeled XRE, and the formation of AhR/Arnt/XRE complexes was analyzed by EMSA. The specificity of binding was determined by incubating the protein treated with TCDD with a 100-fold molar excess of cold XRE. The arrow indicates the specific shift representing the AhR/Arnt/XRE complex. This pattern of AhR alteration was observed in three separate experiments, and only one is shown.

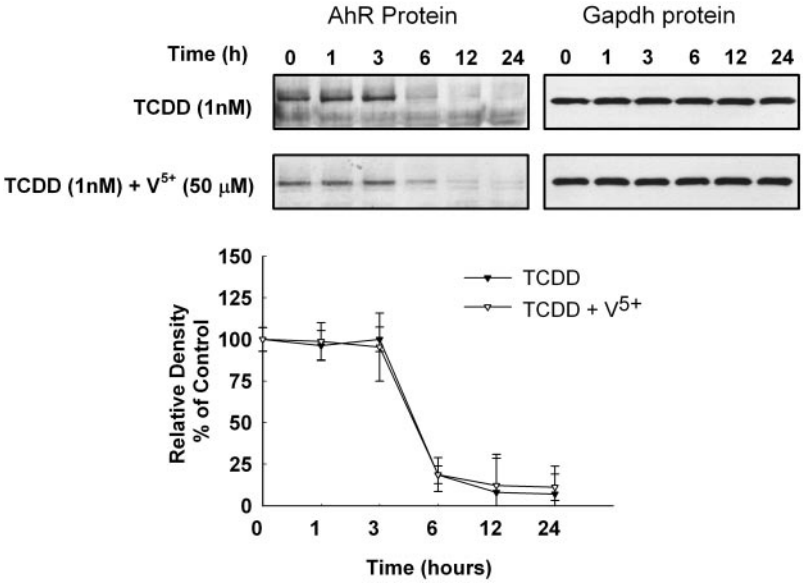

FIG. 6. Time-dependent effect of V^{5+} on AhR protein. Hepa 1c1c7 cells were treated with 1 nM TCDD for the time points indicated in the absence and presence of 50 μM V^{5+}. Protein (25 μg) was separated on a 10% SDS-PAGE and transferred to nitrocellulose membrane. Protein blots were then blocked overnight at 4°C and then incubated with a primary AhR antibody overnight at 4°C, followed by 2 h incubation with secondary antibody at room temperature. AhR protein was detected using the enhanced chemiluminescence method. The intensity of bands was normalized to Gapdh signals, which was used as loading control. The graph represents Gapdh-standardized densitometric readings for AhR protein expressed as a percentage of AhR protein levels of control (time = 0 h) (which is set at 100%) ± S.E. (n = 3).

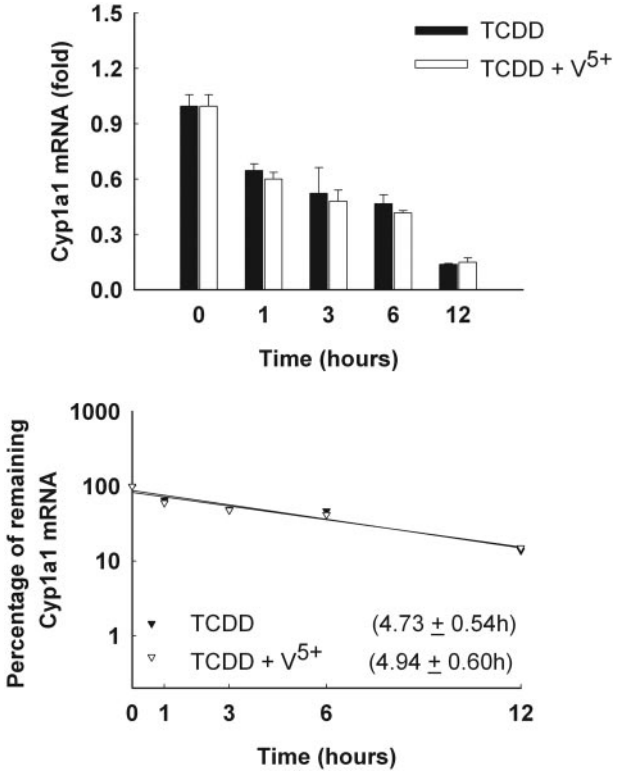

FIG. 7. Effect of V^{5+} on Cyp1a1 mRNA half-life using real-time PCR. Hepa 1c1c7 cells were grown to 90% confluence in six-well cell culture plates and were treated with 1 nM TCDD for 12 h. The cells were then washed and incubated in fresh media containing 50 μM V^{5+} plus 5 μg/ml Act-D, a RNA synthesis inhibitor. First-strand cDNA was synthesized from total RNA (1 μg) extracted from Hepa 1c1c7 cells. cDNA fragments were amplified and quantitated using an ABI 7500 real-time PCR system as described under *Materials and Methods*. Duplicate reactions were performed for each experiment, and the values presented are the means of three independent experiments. mRNA decay curves were analyzed individually, and the half-life was estimated from the slope of a straight line fitted by linear regression analysis ($r^2 \geq 0.85$) to a semilog plot of mRNA amount, expressed as a percentage of treatment at time = 0 h (maximum, 100%) level, versus time. The half-lives obtained from three independent experiments were then used to calculate the mean half-life (mean ± S.E., n = 3). *, $p < 0.05$ compared with TCDD.

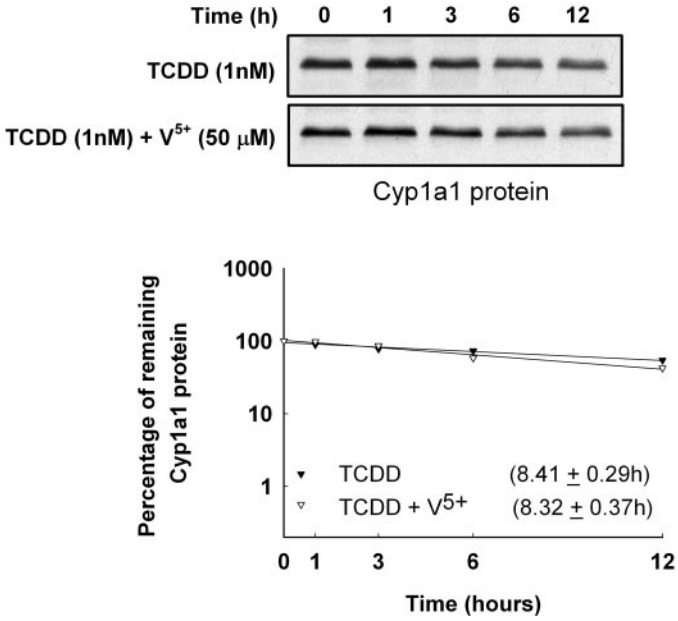

FIG. 8. Effect of V^{5+} on the Cyp1a1 protein half-life. Hepa 1c1c7 cells were grown to 70% confluence in six-well cell culture plates and then were treated with 1 nM TCDD for 24 h. Thereafter, the cells were washed and incubated in fresh media containing 50 μM V^{5+} plus 10 μg/ml CHX, a protein translation inhibitor. Cyp1a1 protein was extracted at the designated time points after the addition of CHX. Protein (25 μg) was separated by 10% SDS-PAGE and transferred to a nitrocellulose membrane. Protein blots were then blocked overnight at 4°C and incubated with a primary polyclonal Cyp1a1 antibody for 2 h at 4°C, followed by 1 h of incubation with secondary monoclonal Cyp1a1 antibody at room temperature. Antibody was detected using the enhanced chemiluminescence method. The intensities of Cyp1a1 protein bands were normalized to Gapdh signals, which were used as loading controls (data not shown). All protein decay curves were analyzed individually. The half-life was estimated from the slope of a straight line fitted by linear regression analysis ($r^2 \geq 0.85$) to a semilog plot of protein amount, expressed as a percentage of treatment at time = 0 h (maximum, 100%) level, versus time. The half-lives obtained from three independent experiments were then used to calculate the mean half-life (mean ± S.E., n = 3). *, $p < 0.05$ compared with TCDD.

failed to produce any significant change in the total cellular heme content (Fig. 9B). Taken together these results exclude any role for V^{5+} in decreasing Cyp1a1 function through decreasing its heme content.

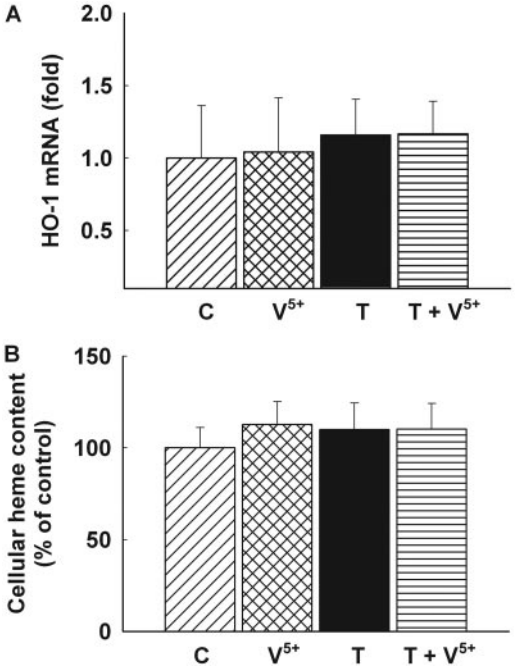

FIG. 9. Effect of V^{5+} on HO-1 mRNA (A) and total cellular heme content (B). A, Hepa 1c1c7 cells were treated for 6 h with 50 μM V^{5+} in the presence and absence of 1 nM TCDD. First-strand cDNA was synthesized from total RNA (1 μg) extracted from Hepa 1c1c7 cells. cDNA fragments were amplified and quantitated using ABI 7500 real-time PCR system as described under *Materials and Methods*. Duplicate reactions were performed for each experiment, and the values presented are the means of three independent experiments. +, $P < 0.05$, compared with control (C) (concentration = 0 μM); *, $P < 0.05$, compared with respective TCDD (T) treatment. B, Hepa 1c1c7 cells were treated for 24 h with 50 μM V^{5+} in the presence and absence of 1 nM TCDD. Thereafter, cells were pelleted and boiled in oxalic acid, followed by resuspension in PBS. After centrifugation, the fluorescence of protoporphyrin IX was assayed by a spectrophotometric method. +, $P < 0.05$, compared with control (C) (concentration = 0 μM); *, $P < 0.05$, compared with respective TCDD (T) treatment.

Effect of Coexposure to V^{5+} and TCDD on Ecto-ATPase Enzymatic Activity. To further investigate how V^{5+} inhibited the AhR/Arnt/XRE binding we examined the effect of coexposure to V^{5+} and TCDD on activity of ecto-ATPase, an enzyme responsible for the conversion of ATP and ADP to AMP, releasing free energy, which is required for AhR translocation. Previous studies have shown that the translocation of the AhR to the nucleus is an ATP-dependent mechanism (Wang and Safe, 1994). To examine the effect of V^{5+} on ecto-ATPase, Hepa 1c1c7 cells were treated with vehicle, V^{5+}, TCDD, or V^{5+} and TCDD for 6 h. Our results show that TCDD alone significantly increased the ecto-ATPase activity, compared with the control (Fig. 10). On the other hand, V^{5+} alone caused a significant decrease in ecto-ATPase activity by ~30% compared with the control. Interestingly, coexposure to V^{5+} and TCDD significantly decreased the ecto-ATPase activity by ~70% compared with TCDD alone (Fig. 10).

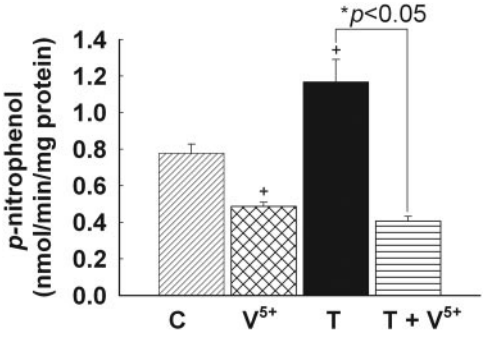

FIG. 10. Effect of coexposure to V^{5+} and TCDD on ecto-ATPase activity. Ecto-ATPase activity was measured in intact living cells treated with increasing concentrations of V^{5+}, in the absence and presence of 1 nM TCDD for 24 h. Ecto-ATPase activity was measured using *p*-nitrophenyl phosphate as a substrate. Values are presented as mean ± S.E. ($n = 6$). +, $P < 0.05$, compared with control (C); *, $P < 0.05$, compared with respective TCDD (T) treatment.

Discussion

Humans consume appreciable amounts of V^{5+} in food and water (Evangelou, 2002). The estimated daily intake of V^{5+} is 10 to 60 μg (Nechay, 1984). In addition, V^{5+} supplements in the form of 10-mg tablets are available from several commercial sources that promote V^{5+} as a body-building supplement. An estimate of the total body pool of vanadium in healthy individuals is 100 to 200 μg (Byrne and Kosta, 1978). If we take into consideration the fact that heavy metals such as V^{5+} are significantly deposited in hepatocytes and kidneys (Edel and Sabbioni, 1989), the concentrations used in the current study are of great relevance to those in humans.

During the last few years, V^{5+} compounds have been shown to be effective in inhibiting cancers of the liver (Bishayee and Chatterjee, 1995), lung, breast, and gastrointestinal tract (Köpf-Maier, 1987; Kanna et al., 2003, 2004). The mechanism for this anticancer effect is not known. However, previous studies have demonstrated that V^{5+} compounds exert protective effects against chemical-induced carcinogenesis mainly by modifying various xenobiotic-metabolizing enzymes (Evangelou, 2002). Data from our laboratory and others showed that heavy metals other than V^{5+} are capable of modifying the carcinogen-metabolizing enzyme, Cyp1a1, at different stages of its regulatory pathway (Bessette et al., 2005; Korashy and El-Kadi, 2005; Elbekai and El-Kadi, 2007; Khan et al., 2007).

In the current study, we hypothesize that V^{5+} protects against TCDD-mediated toxicity and carcinogenicity by inhibiting *Cyp1a1* gene expression. Hence, the main objective of the current study was to determine the potential effects of coexposure to V^{5+} and TCDD on the expression of Cyp1a1. We also explored the molecular mechanism(s) by which V^{5+} modulates the expression of Cyp1a1.

Cyp1a1 gene expression involves the activation of a cytosolic transcriptional factor, the AhR, as the first step in a series of molecular events promoting *Cyp1a1* transcription and translation processes (Denison et al., 1989). Initially, we showed that V^{5+} inhibits TCDD-mediated induction of Cyp1a1 mRNA in a concentration-dependent manner and that this inhibition was further translated to protein and catalytic activity levels. Hepa 1c1c7 cells coexposed to increasing concentrations of V^{5+} and 1 nM TCDD showed a significant dose-dependent inhibition of Cyp1a1 mRNA starting at 25 μM V^{5+} and reaching maximum inhibition at 250 μM.

The transcriptional regulation of *Cyp1a1* gene expression by V^{5+} was supported by a series of indications. V^{5+} inhibited TCDD-mediated induction of AhR-dependent luciferase reporter gene expression (Fig. 4). Thus, V^{5+} either inhibited the transformation of AhR to its DNA-binding form and/or the nuclear accumulation of liganded AhR, thus causing inhibition of AhR/Arnt/XRE complex formation. To determine whether V^{5+} alters Cyp1a1 by interfering with AhR/Arnt/XRE binding, we performed EMSA using nuclear extracts of treated Hepa 1c1c7 cells and untreated guinea pig hepatic cytosol, as described previously (Denison et al., 2002). Our results showed that although V^{5+} failed to inhibit in vitro TCDD-mediated transformation of AhR to its DNA-binding in guinea pig cytosol, it completely abolished the nuclear accumulation of the AhR and its subsequent binding in vivo.

Previous data have shown that liganded AhR is ubiquinated before its degradation by the 26S proteasomal pathway (Pollenz, 2002). To determine whether or not the decrease in AhR/Arnt/XRE binding is due to an increase in the degradation of the AhR protein by V^{5+}, we examined the effect of V^{5+} on AhR protein levels at different time points. Our results showed that AhR degrades rapidly after exposure to TCDD, and at 6 h the remaining AhR was ~15% compared with control (time = 0 h). Coexposure to V^{5+} and TCDD did not significantly alter the AhR protein levels compared with TCDD alone. These results suggest that the observed inhibitory effect of V^{5+} on AhR/Arnt/XRE binding is not due to a decrease in the cellular level of the AhR protein.

We have shown previously that heavy metals modulate Cyp1a1 through transcriptional, post-transcriptional, and post-translational mechanisms (Korashy and El-Kadi, 2005; Elbekai and El-Kadi, 2007). Thus, it was of great importance to determine the effect of V^{5+} on the post-transcriptional regulation of Cyp1a1. The cellular mRNA level at any time point is a function of the rate of its production, through a transcriptional mechanism, and the rate of its degradation. Therefore, we examined the effect of V^{5+} on the stability of Cyp1a1 mRNA using the Act-D chase experiment. Our results showed that Cyp1a1 mRNA induced by TCDD is short-lived, with an estimated half-life of 4.73 ± 0.54 h. Our results are in agreement with previous reports showing that the half-life of Cyp1a1 mRNA induced by TCDD in Hepa 1c1c7 cells ranges from 3 to 4.5 h (Miller et al., 1983; Chen et al., 1995). On the other hand, V^{5+} did not significantly alter the stability of Cyp1a1 mRNA, suggesting that a post-transcriptional mechanism is not involved in the modulation of Cyp1a1 mRNA by V^{5+}.

To examine the effect of coexposure to V^{5+} and TCDD at the post-translational level, a CHX chase experiment was performed. Our results showed that the Cyp1a1 protein induced by TCDD has an estimated half-life of 8.41 ± 0.29 h. In contrast, V^{5+} did not significantly alter the stability of Cyp1a1 protein, inferring that a post-translational mechanism is not involved in the modulation of Cyp1a1 protein by V^{5+}.

Our previous studies have shown that heavy metals possess the ability to decrease Cyp1a1 activity through an effect on its heme content (Korashy and El-Kadi, 2005; Elbekai and El-Kadi, 2007). These results prompted us to examine the effect of coexposure to V^{5+} and TCDD on HO-1 mRNA and total cellular heme content. In the current study we showed that V^{5+} did not significantly alter the HO-1 mRNA level and total cellular heme content. Thus, these results exclude any possibility that V^{5+} might have decreased Cyp1a1 activity through affecting its heme content.

It has been reported previously that V^{5+} is capable of activating the redox-sensitive transcription factor, nuclear factor-κB (NF-κB) (Chen et al., 2001). Of interest, it has been demonstrated that there is a mutual inhibitory interaction between the AhR and the NF-κB signaling pathways (Ke et al., 2001). The possibility that NF-κB prevents AhR/Arnt binding to the XRE is excluded, because it has been shown that NF-κB activation does not affect AhR/Arnt binding to XRE (Ke et al., 2001). Therefore, the inhibitory effect of V^{5+} on AhR/Arnt/XRE binding is NF-κB-independent.

Although V^{5+} has been known since 1965 to inhibit ATPases (Nechay, 1984), few studies have been conducted to examine its effect on ecto-ATPase, the main enzyme responsible for releasing energy from ATP (Wood et al., 2002) that would be used by the liganded AhR for nuclear translocation (Wang and Safe, 1994). Interestingly, previous studies using high concentrations of V^{5+} (1 mM) showed that V^{5+} affects the translocation of the AhR to the nucleus by inhibiting ATPases (Wang and Safe, 1994). These findings prompted us to investigate the possible role of ecto-ATPase in the modulation of Cyp1a1 by V^{5+}. In this study we have shown that V^{5+} decreased ecto-ATPase enzymatic activity. These results are in agreement with previous studies (Wang and Safe, 1994) that have reported an ATP-dependent mechanism for the inhibition of AhR translocation by V^{5+}. These results suggest that the ability of V^{5+} to inhibit AhR transformation and hence XRE binding is due to its effect on ecto-ATPase catalytic activity.

In conclusion, the present study demonstrates that V^{5+} down-regulates the bioactivating enzyme Cyp1a1 through a transcriptional mechanism. The translocation of the transformed AhR was inhibited by V^{5+} probably by inhibiting ecto-ATPase activity. Thus, these results suggest that V^{5+} may protect against TCDD-mediated toxicity by inhibiting *Cyp1a1* gene expression. However, further studies are needed to investigate the cytoprotective effect of V^{5+} against TCDD-mediated toxicity.

Acknowledgments. We are grateful to Dr. M. S. Denison (University of California, Davis, Davis, CA) for providing us with XRE-luciferase reporter plasmid pGudLuc1.1 and guinea pig hepatic cytosol.

References

Anagnostou F, Plas C, and Forest N (1996) Ecto-alkaline phosphatase considered as levamisole-sensitive phosphohydrolase at physiological pH range during mineralization in cultured fetal calvaria cells. *J Cell Biochem* **60:**484–494.

Anwar-Mohamed A and El-Kadi AO (2007) Induction of cytochrome P450 1a1 by the food flavoring agent, maltol. *Toxicol In Vitro* **21:**685–690.

Behnisch PA, Hosoe K, and Sakai S (2001) Bioanalytical screening methods for dioxins and dioxin-like compounds a review of bioassay/biomarker technology. *Environ Int* **27:**413–439.

Bessette EE, Fasco MJ, Pentecost BT, and Kaminsky LS (2005) Mechanisms of arsenite-mediated decreases in benzo[*k*]fluoranthene-induced human cytochrome P4501A1 levels in HepG2 cells. *Drug Metab Dispos* **33:**312–320.

Bishayee A and Chatterjee M (1995) Inhibitory effect of vanadium on rat liver carcinogenesis initiated with diethylnitrosamine and promoted by phenobarbital. *Br J Cancer* **71:**1214–1220.

Bohonowych JE, and Denison MS (2007) Persistent binding of ligands to the aryl hydrocarbon receptor. *Toxicol Sci* **98:**99–109.

Byrne AR and Kosta L (1978) Vanadium in foods and in human body fluids and tissues. *Sci Total Environ* **10:**17–30.

Cantley LC Jr and Aisen P (1979) The fate of cytoplasmic vanadium: implications on (Na,K)-ATPase inhibition. *J Biol Chem* **254:**1781–1784.

Chen F, Ding M, Castranova V, and Shi X (2001) Carcinogenic metals and NF-κB activation. *Mol Cell Biochem* **222:**159–171.

Chen YH, Riby J, Srivastava P, Bartholomew J, Denison M, and Bjeldanes L (1995) Regulation of CYP1A1 by indolo[3,2-*b*]carbazole in murine hepatoma cells. *J Biol Chem* **270:**22548–22555.

Denison MS, Fisher JM, and Whitlock JP Jr (1989) Protein-DNA interactions at recognition sites for the dioxin-Ah receptor complex. *J Biol Chem* **264:**16478–16482.

Denison MS, Pandini A, Nagy SR, Baldwin EP, and Bonati L (2002) Ligand binding and activation of the Ah receptor. *Chem Biol Interact* **141:**3–24.

Edel J and Sabbioni E (1989) Vanadium transport across placenta and milk of rats to the fetus and newborn. *Biol Trace Elem Res* **22:**265–275.

Elbekai RH and El-Kadi AO (2004) Modulation of aryl hydrocarbon receptor-regulated gene expression by arsenite, cadmium, and chromium. *Toxicology* **202:**249–269.

Elbekai RH and El-Kadi AO (2007) Transcriptional activation and posttranscriptional modification of Cyp1a1 by arsenite, cadmium, and chromium. *Toxicol Lett* **172:**106–119.

Evangelou AM (2002) Vanadium in cancer treatment. *Crit Rev Oncol Hematol* **42:**249–265.

Hankinson O (1995) The aryl hydrocarbon receptor complex. *Annu Rev Pharmacol Toxicol* **35:**307–340.

Kanna PS, Mahendrakumar CB, Chatterjee M, Hemalatha P, Datta S, and Chakraborty P (2003) Vanadium inhibits placental glutathione S-transferase (GST-P) positive foci in 1,2-dimethyl hydrazine induced rat colon carcinogenesis. *J Biochem Mol Toxicol* **17:**357–365.

Kanna PS, Mahendrakumar CB, Indira BN, Srivastawa S, Kalaiselvi K, Elayaraja T, and Chatterjee M (2004) Chemopreventive effects of vanadium toward 1,2-dimethylhydrazine-induced genotoxicity and preneoplastic lesions in rat colon. *Environ Mol Mutagen* **44:**113–118.

Ke S, Rabson AB, Germino JF, Gallo MA, and Tian Y (2001) Mechanism of suppression of cytochrome P-450 1A1 expression by tumor necrosis factor-α and lipopolysaccharide. *J Biol Chem* **276:**39638–39644.

Khan S, Liu S, Stoner M, and Safe S (2007) Cobaltous chloride and hypoxia inhibit aryl hydrocarbon receptor-mediated responses in breast cancer cells. *Toxicol Appl Pharmacol* **223:**28–38.

Köpf-Maier P (1987) Cytostatic non-platinum metal complexes: new perspectives for the treatment of cancer? *Naturwissenschaften* **74:**374–382.

Korashy HM and El-Kadi AO (2005) Regulatory mechanisms modulating the expression of cytochrome P450 1A1 gene by heavy metals. *Toxicol Sci* **88:**39–51.

Korashy HM and El-Kadi AO (2008) Modulation of TCDD-mediated induction of cytochrome P450 1A1 by mercury, lead, and copper in human HepG2 cell line. *Toxicol In Vitro* **22:**154–158.

Kransler KM, McGarrigle BP, and Olson JR (2007) Comparative developmental toxicity of

2,3,7,8-tetrachlorodibenzo-*p*-dioxin in the hamster, rat and guinea pig. *Toxicology* **229:**214–225.
Lorenzen A, and Kennedy SW (1993) A fluorescence-based protein assay for use with a microplate reader. *Anal Biochem* **214:**346–348.
Lowry OH, Rosebrough NJ, Farr AL, and Randall RJ (1951) Protein measurement with the Folin phenol reagent. *J Biol Chem* **193:**265–275.
Maniratanachote R, Minami K, Katoh M, Nakajima M, and Yokoi T (2005) Chaperone proteins involved in troglitazone-induced toxicity in human hepatoma cell lines. *Toxicol Sci* **83:**293–302.
Meyer BK, Pray-Grant MG, Vanden Heuvel JP, and Perdew GH (1998) Hepatitis B virus X-associated protein 2 is a subunit of the unliganded aryl hydrocarbon receptor core complex and exhibits transcriptional enhancer activity. *Mol Cell Biol* **18:**978–988.
Miller AG, Israel D, and Whitlock JP Jr (1983) Biochemical and genetic analysis of variant mouse hepatoma cells defective in the induction of benzo(*a*)pyrene-metabolizing enzyme activity. *J Biol Chem* **258:**3523–3527.
Nebert DW, Dalton TP, Okey AB, and Gonzalez FJ (2004) Role of aryl hydrocarbon receptor-mediated induction of the CYP1 enzymes in environmental toxicity and cancer. *J Biol Chem* **279:**23847–23850.
Nebert DW and Duffy JJ (1997) How knockout mouse lines will be used to study the role of drug-metabolizing enzymes and their receptors during reproduction and development, and in environmental toxicity, cancer, and oxidative stress. *Biochem Pharmacol* **53:**249–254.
Nechay BR (1984) Mechanisms of action of vanadium. *Annu Rev Pharmacol Toxicol* **24:**501–524.
Pollenz RS (2002) The mechanism of AH receptor protein down-regulation (degradation) and its impact on AH receptor-mediated gene regulation. *Chem Biol Interact* **141:**41–61.
Rojas E, Herrera LA, Poirier LA, and Ostrosky-Wegman P (1999) Are metals dietary carcinogens? *Mutat Res* **443:**157–181.
Schrenk D (1998) Impact of dioxin-type induction of drug-metabolizing enzymes on the metabolism of endo- and xenobiotics. *Biochem Pharmacol* **55:**1155–1162.
Wang X and Safe S (1994) Development of an in vitro model for investigating the formation of the nuclear Ah receptor complex in mouse Hepa 1c1c7 cells. *Arch Biochem Biophys* **315:**285–292.
Ward JH, Jordan I, Kushner JP, and Kaplan J (1984) Heme regulation of HeLa cell transferrin receptor number. *J Biol Chem* **259:**13235–13240.
Whitelaw ML, Gustafsson JA, and Poellinger L (1994) Identification of transactivation and repression functions of the dioxin receptor and its basic helix-loop-helix/PAS partner factor Arnt: inducible versus constitutive modes of regulation. *Mol Cell Biol* **14:**8343–8355.
Wood E, Johan Broekman M, Kirley TL, Diani-Moore S, Tickner M, Drosopoulos JH, Islam N, Park JI, Marcus AJ, and Rifkind AB (2002) Cell-type specificity of ectonucleotidase expression and upregulation by 2,3,7,8-tetrachlorodibenzo-*p*-dioxin. *Arch Biochem Biophys* **407:**49–62.

Address correspondence to: Dr. Ayman O. S. El-Kadi, Faculty of Pharmacy and Pharmaceutical Sciences, 3126 Dentistry/Pharmacy Centre, University of Alberta, Edmonton, AB, Canada T6G 2N8. E-mail: aelkadi@pharmacy.ualberta.ca